Ionospheric gravity waves detected offshore Hawaii after tsunamis

Lucie M. Rolland,[1] Giovanni Occhipinti,[1] Philippe Lognonné,[1] and Anne Loevenbruck[2]

Received 26 June 2010; accepted 28 July 2010; published 1 September 2010.

[1] On-board satellites techniques provide global coverage and could play an important role in the continuous oceanic survey to prevent the damage produced by powerful tsunamis. We report here new ionospheric observations related to three significant transpacific tsunami events triggered by the 2006 Kuril earthquake, the 2009 Samoa earthquake and the 2010 Chile earthquake. Total Electron Content (TEC) variations extracted from data recorded by a dense Global Positioning System (GPS) network based in Hawaii show ionospheric disturbances within the hours following the tsunami wave passage at sea-level. For each event, we observe ionospheric gravity waves propagating with velocity, direction and arrival time coherent with the tsunami. The tsunamigenic signature in the ionosphere is also compared to in-situ sea-level measurements. These observations provide new examples of the sensitivity of the ionosphere to tsunamigenic gravity waves and confirm that ionospheric monitoring by GPS can provide complementary information on tsunami propagation. **Citation:** Rolland, L. M., G. Occhipinti, P. Lognonné, and A. Loevenbruck (2010), Ionospheric gravity waves detected offshore Hawaii after tsunamis, *Geophys. Res. Lett.*, *37*, L17101, doi:10.1029/2010GL044479.

1. Introduction

[2] Early studies about propagation of internal gravity waves (IGW) during the seventies have suggested that the ionosphere is sensitive to IGW by the forcing effect of a tsunami on the surrounding atmosphere [*Hines*, 1972]. The upward propagating atmospheric wave is amplified as the air density decreases, then reaches the ionospheric heights and exchanges a part of its energy with the charged particles by coupling mechanisms. *Peltier and Hines* [1976] inferred that these gravity waves might be detectable and used for tsunami warning system purpose.

[3] Taking advantage of the dense Japanese Global Positioning System (GPS) network GEONET, *Artru et al.* [2005] detected for the first time the propagation of Total Electron Content (TEC) perturbations consistent with the propagation of a tsunami. This was triggered by the 23 June 2001 Mw 8.2 earthquake in Peru. TEC is the electron density integrated along the satellite-ground station line-of-sight and commonly measured in TEC units (1 $TECU = 10^{16}$ *electrons*/m^2). TEC enables the mapping of ionospheric perturbations in the case of dense GPS networks [*Lognonné et al.*, 2006]. However, the TEC perturbations observed by *Artru et al.* [2005] had a low signal-to-noise ratio due to the small amplitude of the tsunami in the open-ocean (a few cm near Japan) as well as to several medium-scale Traveling Ionospheric Disturbances (TIDs) superimposed to the tsunamigenic signal.

[4] The giant Sumatran 2004 Mw 9.2 earthquake and the related tsunami was 20 times more energetic than the Peruvian one and exceptional ionospheric signals were recorded worldwide [*Liu et al.*, 2006a, 2006b; *DasGupta et al.*, 2006]. The altimeters Jason-1 and Topex/Poseidon were crossing the Indian ocean 2 hours after the seismic rupture and provided simultaneous TEC and sea-level measurements. The observed TEC signatures were first reproduced by *Occhipinti et al.* [2006] using a synthetic sea-level displacement as input of a gravity wave propagation model. This result, also confirmed by *Mai and Kiang* [2009], proved the link between the tsunami and the ionospheric disturbances. More complex effects such as the directivity related to the magnetic field and the high altitude attenuation of gravity waves were modeled respectively by *Occhipinti et al.* [2008] and by *Hickey et al.* [2009].

[5] We present here three occurrences of far-field ionospheric perturbations offshore Hawaii, following three significant tsunami events triggered by earthquakes located in three different geographical directions, as shown on Figure 1a: Northwest, the Mw 8.3 earthquake on 15 November 2006 in Kuril island, Southwest, the Mw 8.1 earthquake on 29 September 2009 in the Samoa islands region and Southeast, the Mw 8.8 earthquake on 27 February 2010 in central Chile.

[6] The proper geometry of GPS satellites allowed offshore TEC observations induced by the tsunami propagation at several hundreds of kilometers from the Hawaiian coasts. The TEC observations are also supported by in-situ sea-level measurements.

[7] These observations strongly confirm the idea that ionospheric sounding could be particularly decisive for tsunami warning, particularly in the Hawaiian coastlines that experienced in the past destructive tsunamis.

2. Observations

[8] The US Geological Survey (http://earthquake.usgs.gov/) reports that the Mw 8.3 Kuril earthquake occurred at 01:14:17 AM in Hawaii Standard Time (HST) as thrust-faulting on the boundary between the Pacific plate and the Okhotsk plate. The tsunami wave reached the Hawaiian islands about 6 hours later with a maximum amplitude of 2.8 cm measured by the DART (Deep-Ocean Assessment and Reporting of Tsunami) buoy 51406 off Hawaii Island (Figure 1b). The resonant amplifications due to the coastal topography explain the comparatively high amplitude of 76 cm recorded by a tide-gauge in Kahului harbor [*Munger and Cheung*, 2008].

[9] The Mw 8.1 Samoan earthquake occurred at 07:48:11 AM (HST) and triggered a powerful and damaging tsunami

[1]Géophysique Spatiale et Planétaire, Institut de Physique du Globe de Paris, Université Paris Diderot, UMR CNRS 7154, Saint-Maur des Fossés, France.
[2]Commissariatà l'Énergie Atomique, DAM-DIF, Arpajon, France.

0094-8276/10/2010GL044479

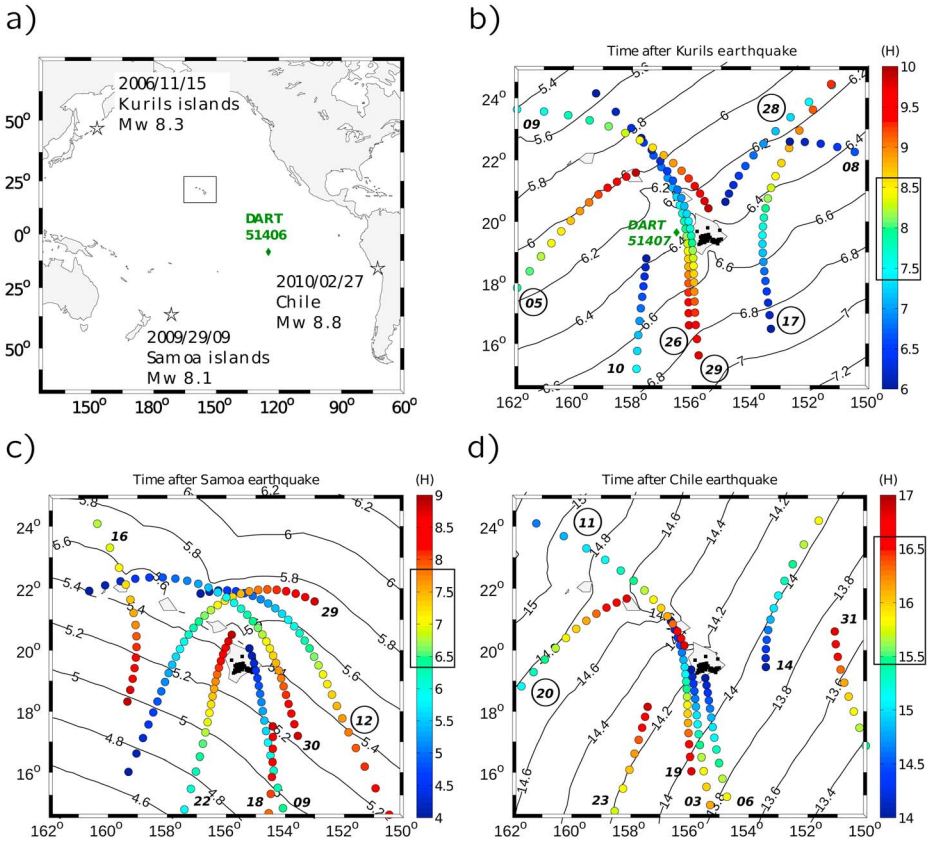

Figure 1. (a) Epicenter locations of the 3 tsunami events investigated in the present study. The Hawaii region is highlighted by a rectangle. (b–d) Observation geometry of Kuril 2006, Samoa 2009 and Chile 2010 respectively. Ionospheric sounding points (IPPs) at 300 km height for GPS receiver KNNE and visible satellites are located every 10 minutes. The most significant perturbations are observed by GPS satellites with encircled number during the time range marked by a rectangle on the colorbar. IPPs are superimposed to the tsunami travel time map of the event, modeled using the TTT software (Tsunami Travel Time [*Wessel*, 2009]) and USGS source. The black squares show the locations of the whole GPS ground receivers used in the study.

that hit Samoa, American Samoa, and Tonga a few tens minutes later. Tsunami run-ups larger than 3 meters were observed in American Samoa (USGS). Six hours after the seismic event, the tsunami wave reaching the Hawaiian archipelago was much more moderate: tide-gauges measured run-ups of a few tens of centimeters. The modeled sea-level displacement in deep ocean next to Hawaii does not exceed 2 cm according to NOAA (http://www.noaa.gov/samoa20090929/).

[10] Much more powerful, the Mw 8.8 Chile earthquake occurred at 08:34:14 PM (HST). The maximum wave height was estimated by NOAA to about 10 cm offshore Hawaii, so that a large-scale evacuation was organized by the authorities. However the tsunami caused minimal damages on the Hawaiian coasts, reached about 14 hours after the earthquake. The tide-gauges measured sea-level did not exceed 89 cm in amplitude.

[11] We collected 30s-sampled data from about 50 GPS permanent ground stations from the public websites of the SOPAC (http://sopac.ucsd.edu/) and UNAVCO (http://www.unavco.org/). Following *Mannucci et al.* [1998], a biased slant TEC time-series is calculated from the L1 and L2 carrier phases difference, for each satellite-ground station pair. The TEC values are corrected from the satellite elevation angle after [*Artru et al.*, 2005]. The vertical TEC (vTEC) daily variations are then removed by high-pass filtering [*Artru et al.*, 2005] and gravity waves are highlighted using a Butterworth filter with 1 to 5 mHz frequency bandwidth. Each vTEC measurement is assumed to be located at the Ionospheric Pierce Point (IPP). As shown on Figure S1 of the auxiliary material[1], this point is the intersection of the satellite-station ray-path with a thin shell located at 300 km height. The vertical projection of IPP at sea-level is the Sub-Ionospheric Point (SIP).

[12] Although several satellites were visible (Figure 1), only a couple of satellites detected ionospheric waves with significant signal-noise ratio during the interval of the tsunami propagation near Hawaii. Figure 2a shows the sounding IPPs after the passage of the tsunami, in essence the projection of the Hawaiian GPS network along the line-of-sight to the GPS satellites. The satellites detecting the most significant perturbations (see Table 1) have low elevation angles and azimuths that enable the constructive integration of the tsunamigenic ionospheric waves [*Artru et al.*, 2005; *Occhipinti et al.*, 2008; *Hickey et al.*, 2009].

[13] In order to exclude any recurrent TIDs and systematic multi-path, we verified that the ionospheric background was quiet (A_p < 10, see Table 1) and that no significant pertur-

[1]Auxiliary materials are available in the HTML. doi:10.1029/2010GL044479.

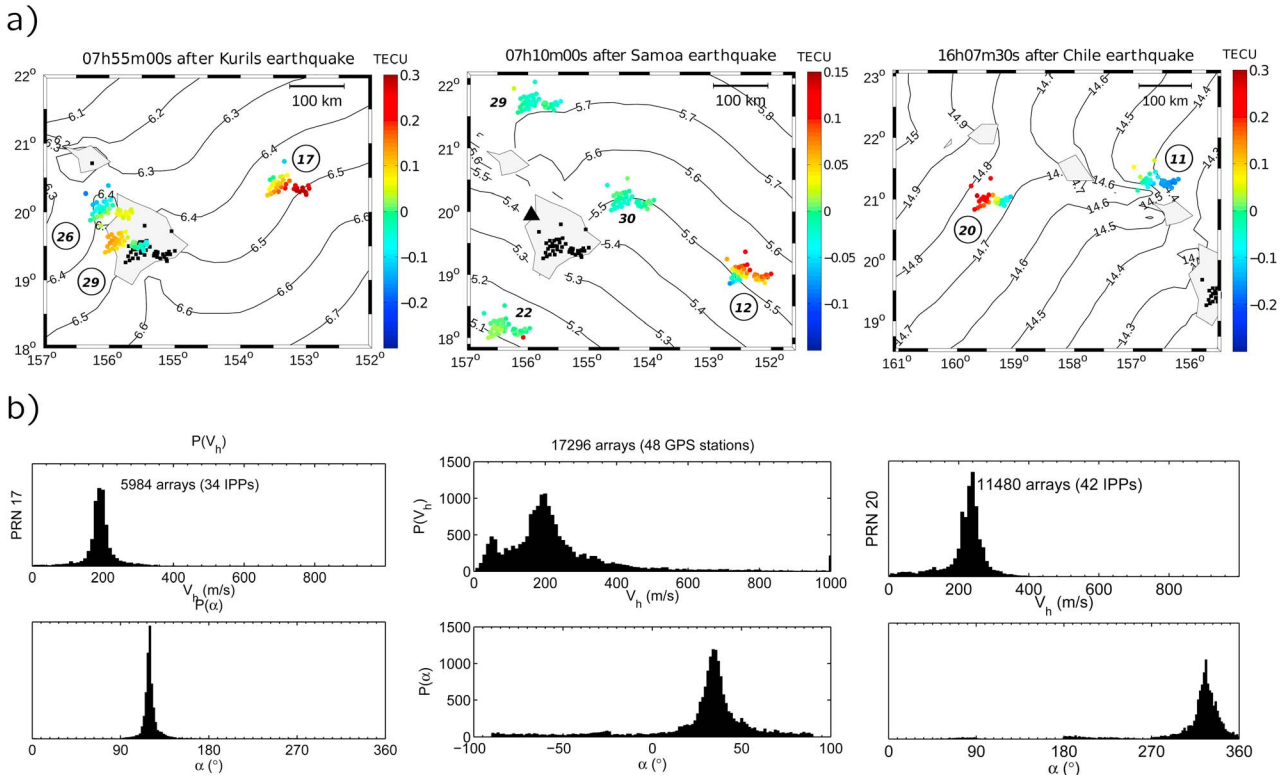

Figure 2. (a) Instantaneous vTEC plotted about 1 hour after the theoretical tsunami arrival at sea-level, from left to right: after Kuril, Samoa and Chile earthquakes respectively. Animations on the full time range of observation are provided as auxiliary material (Animations S1–S3). (b) Corresponding distributions of the propagation parameters, horizontal velocity (V_h) and azimuth angle (α), using a GPS array statistical method [*Afraimovich et al.*, 2004] applied to the maximal vTEC disturbance observed with satellites PRN 17, 12 and 20 respectively.

bation was observed the day before or the day after for the same GPS time interval.

[14] The mapping of the vTEC variations on IPPs (Figure 2b) shows clear wave patterns within 2 hours following the theoretical tsunami arrival time. The lowest maximal zero-to-peak amplitude is observed for the Samoa event (0.15 TECU), less powerful than the Kuril and Chile event, where the amplitude reaches 0.4 TECU and 0.5 TECU respectively.

[15] We use a statistical GPS array method [*Afraimovich et al.*, 2004] to derive the horizontal phase velocity vector independently of the source location. The distributions of azimuth angle (from north toward the east) and propagation speed are depicted on Figure 2b and the resulting estimations are summarized in Table 1. For each event, the azimuth angles are consistent with the tsunami direction of propagation, as well as the propagation speeds over a region where the depth H can reach 6 km, corresponding to a tsunami speed $v = \sqrt{gH}$ = 243 m/s, where g is gravity. We also highlight coherence with the tsunami travel-time model, which is taken as time and space reference: the vTEC perturbations are vertically aligned in the travel-time diagrams on Figure 3.

[16] To additionally support the tsunamigenic signature in the ionosphere, we compare the ionospheric perturbations observed *via* the TEC with the tsunami at sea-level. The closest coastal tide-gauge (Figure 2b) is located in the Kawaihae harbor at the northwest coast of the Hawaii Island. The closest DART buoy (51406) is located 50 km west of Hawaii Island, in open ocean (Figure 1a). After *Munger and Cheung* [2008] it is representative for the open-ocean tsunami approaching from the West. For the Samoa event, the closest functioning DART buoy (51407) was located 5370 km southeast of Hawaii (see Figure 1a). For the Chile event, neither the 51406 buoy nor the 51407 buoy were functioning.

[17] Time-series were collected from NOAA and filtered with the same method and frequency bandwidth used for the

Table 1. Summary of the Tsunami Events Characteristics and GPS-TEC Detection Results[a]

Event	h_{max}	$vTEC_{max}$	v_h	α	PRN	El/Az	T (HST)	A_p
Kuril 2006	2.8 cm (measured)	0.40 TECU	200 m/s	123°	17	50°/65°	09 AM	7
Samoa 2009	2 cm (estimated)	0.15 TECU	200 m/s	35°	12	45°/105°	15 PM	5
Chile 2010	10 cm (estimated)	0.50 TECU	240 m/s	325°	20	35°/300°	01 AM	1

[a] h_{max} is the maximum amplitude of the water height above sea-level measured or estimated in open ocean offshore Hawaii. $vTEC_{max}$ is the maximum vTEC filtered between 1 and 5 mHz and detected using the given GPS satellite PRN number, having El and Az as elevation and azimuth angles. v_h and α are the estimated horizontal propagation speed (±20%) and azimuth angle (±5°) of the perturbation (see Figure 2). T is local time of observations and A_p is the daily geomagnetic disturbance index.

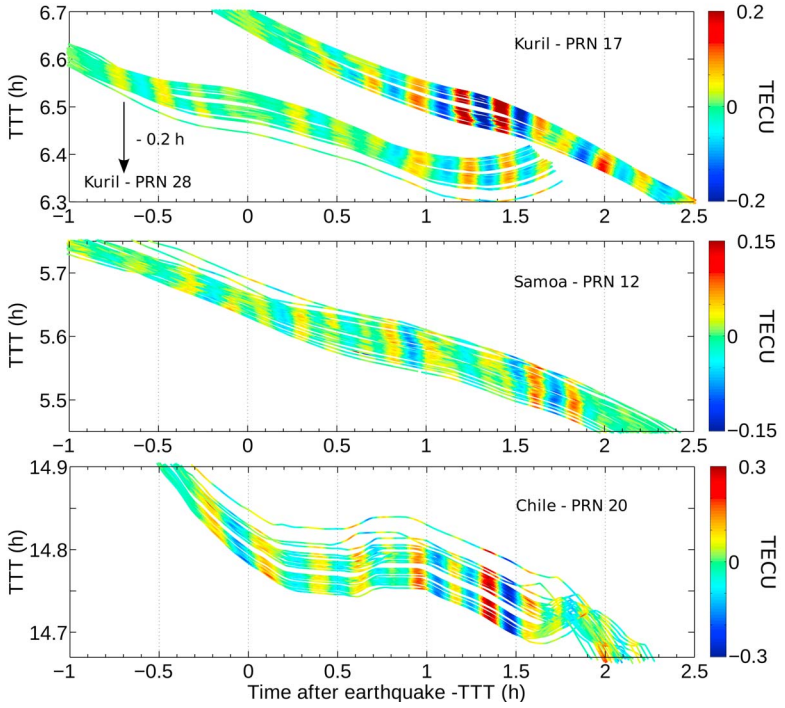

Figure 3. Travel-time diagrams of the vTEC time-series at the time of tsunami arrival off Hawaii, from top to bottom: for Kuril, Samoa and Chile events, respectively. Time is related to the tsunami travel time to highlight coherence with the tsunami model.

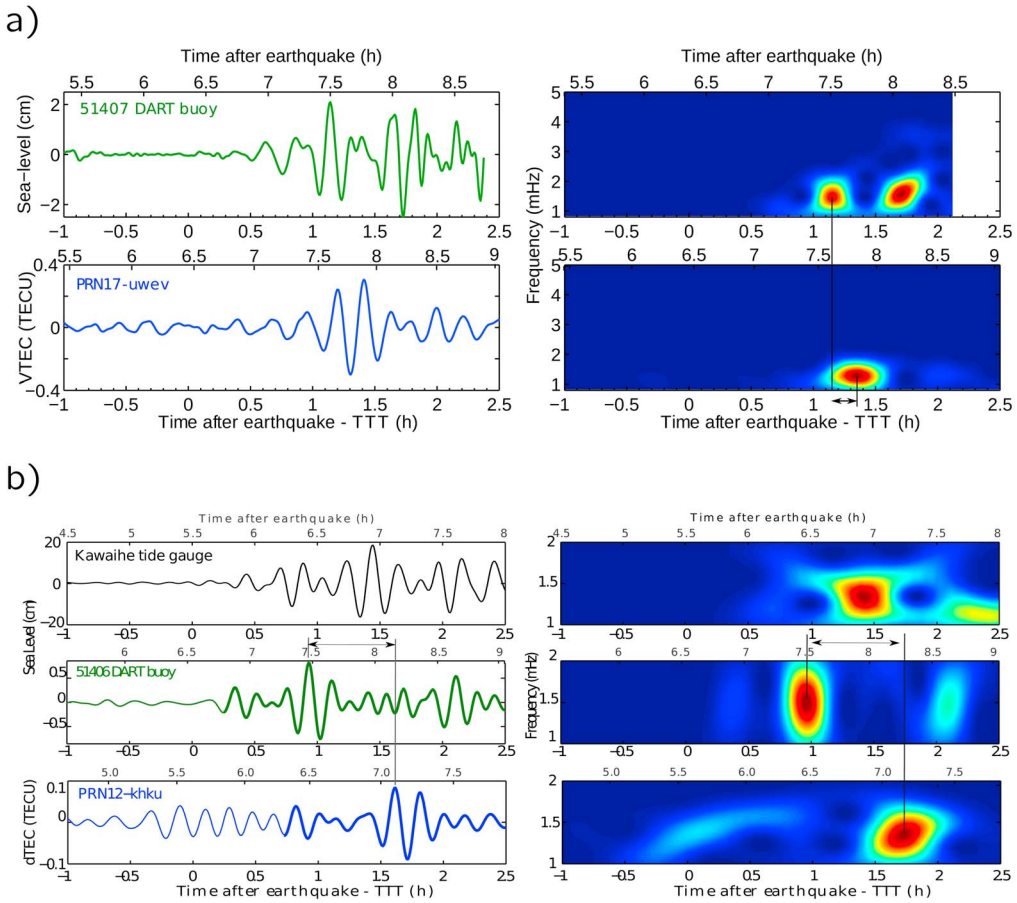

Figure 4. (left) Time series and (right) corresponding spectral-time diagrams. (a) Kuril event band-pass filtering between 1 and 5 mHz. (b) Samoa event, band-pass filtering between 1 and 2 mHz. Black and green curves: sea-level height measured by a coastaltide-gauge and a deep ocean buoy, respectively and blue curve: vTEC detected using the specified GPS station-satellite pair. The arrows provide measurements of the tsunami detection delay by GPS-TEC technique.

TEC time-series (1 to 5 mHz). For the Samoa event, this frequency band is reduced to 1–2 mHz in order to enhance the signal-to-noise-ratio. As shownby Figure 4, the vTEC time series are very similar to the sea-level time series, in waveforms as for the frequency content, with a dominant frequency peak around 1.5 mHz (about 10 minutes) for both events. As a consequence, the observed perturbations arepure gravity waves.

[18] Assuming that far-field tsunami waves in open ocean are linear and non-dispersive, the sea-level measurement made by the DART buoy can be considered as a reference waveform.

[19] Consequently, the observed time delay between the tsunami arrival time at SIP and the tsunami detection in the ionosphere (at IPP) is 12 minutes for the Kuril event and 45 minutes for the Samoa event. The thin shell approximation introduces a 5 minutes uncertainty on this estimation. The 12 minutes estimated delay is coherent with the 8-minutes average delay estimated by *Liu et al.* [2006b] and modeled following *Occhipinti et al.* [2008] for a 1.3 mHz tsunami wave and 5 km bathymetry (Figure S2). For the Samoa event, the measured delay is less significant, as the tsunami propagation model introduces a large uncertainty between the ionospherically sounded area and the very distant DART buoy 51406. This shows however that the observed fluctuations are related to the tsunami wave at sea-level.

3. Conclusion

[20] Using the imaging capabilities offered by the GPS-TEC technique applied to the GPS dense Hawaiian network we show ionospheric perturbations with a horizontal propagation at around 200 m/s, coherent with 3 major tsunami events. The respective observed amplitude ranges and directions of propagation are also consistent.

[21] Comparisons between the TEC perturbations and sea-level observations confirm similarities in the observed period and waveform as well as a ionospheric detection delay of about 10 minutes consistent with previous observations and tsunamigenic internal gravity waves propagation models. After the recent theoretical and observational results related to the Sumatra tsunami [*Occhipinti et al.*, 2006, 2008; *Mai and Kiang*, 2009; *Hickey et al.*, 2009] these observationshighlight furthermore the coupling between tsunamis and the ionosphere. A joint inversion of tsunami wave from such data should take into account important effects as ionosphere dynamics, geomagnetic field and observation geometry.

[22] The Global Navigation Satellite Systems (GNSS) provides offshore observations hundreds of kilometers away

from the coasts. Coupled with sea-level observations and seismic networks, the continuous monitoring of ionosphere by remote sensing could be particularly decisive for tsunami warning and damage limitations.

[23] **Acknowledgments.** We acknowledge the Universities of Hawaii and Stanford and the USGS Hawaii Volcano Observatory as providers of the GPS data. This work was supported by CNES. LR is supported by CNES/NOVELTIS and thanks P. Coïsson for fruitful discussions. We thank two anonymous reviewers for constructive comments. This is IPGP contribution 3058.

References

Afraimovich, E., E. Astafieva, and S. Voyeikov (2004), Isolated ionospheric disturbances as deduced from global GPS network, *Ann. Geophys.*, *22*, 47–62.

Artru, J., V. Ducic, H. Kanamori, P. Lognonné, and M. Murakami (2005), Ionospheric detection of gravity waves induced by tsunamis, *Geophys. J. Int.*, *160*, 840–848, doi:10.1111/j.1365-246X.2005.02552.x.

DasGupta, A., A. Das, D. Hui, K. K. Bandyopadhyay, and M. R. Sivaraman (2006), Ionospheric perturbations observed by the GPS following the December 26th, 2004 Sumatra-Andaman earthquake, *Earth Planets Space*, *58*, 167–172.

Hickey, M. P., G. Schubert, and R. L. Walterscheid (2009), Propagation of tsunami-driven gravity waves into the thermosphere and ionosphere, *J. Geophys. Res.*, *114*, A08304, doi:10.1029/2009JA014105.

Hines, C. O. (1972), Gravity waves in the atmosphere, *Nature*, *239*, 73–78, doi:10.1038/239073a0.

Liu, J. Y., Y. B. Tsai, S. W. Chen, C. P. Lee, Y. C. Chen, H. Y. Yen, W. Y. Chang, and C. Liu (2006a), Giant ionospheric disturbances excited by the M9.3 Sumatra earthquake of 26 December 2004, *Geophys. Res. Lett.*, *33*, L02103, doi:10.1029/2005GL023963.

Liu, J.-Y., Y.-B. Tsai, K.-F. Ma, Y.-I. Chen, H.-F. Tsai, C.-H. Lin, M. Kamogawa, and C.-P. Lee (2006b), Ionospheric GPS total electron content (TEC) disturbances triggered by the 26 December 2004 Indian Ocean tsunami, *J. Geophys. Res.*, *111*, A05303, doi:10.1029/2005JA011200.

Lognonné, P., et al. (2006), Ground-based GPS imaging of ionospheric post-seismic signal, *Planet. Space Sci.*, *54*, 528–540, doi:10.1016/j.pss.2005.10.021.

Mai, C.-L., and J.-F. Kiang (2009), Modeling of ionospheric perturbation by 2004 Sumatra tsunami, *Radio Sci.*, *44*, RS3011, doi:10.1029/2008RS004060.

Mannucci, A. J., B. D. Wilson, D. N. Yuan, C. H. Ho, U. J. Lindqwister, and T. F. Runge (1998), A global mapping technique for GPS-derived ionospheric total electron content measurements, *Radio Sci.*, *33*, 565–582.

Munger, S., and K. F. Cheung (2008), Resonance in Hawaii waters from the 2006 Kuril Islands Tsunami, *Geophys. Res. Lett.*, *35*, L07605, doi:10.1029/2007GL032843.

Occhipinti, G., P. Lognonné, E. A. Kherani, and H. Hébert (2006), Three-dimensional waveform modeling of ionospheric signature induced by the 2004 Sumatra tsunami, *Geophys. Res. Lett.*, *33*, L20104, doi:10.1029/2006GL026865.

Occhipinti, G., E. A. Kherani, and P. Lognonné (2008), Geomagnetic dependence of ionospheric disturbances induced by tsunamigenic internal gravity waves, *Geophys. J. Int.*, *173*, 753–765, doi:10.1111/j.1365-246X.2008.03760.x.

Peltier, W. R., and C. O. Hines (1976), On the possible detection of tsunamis by a monitoring of the ionosphere, *J. Geophys. Res.*, *81*, 1995–2000, doi:10.1029/JC081i012p01995.

Wessel, P. (2009), Analysis of observed and predicted tsunami travel times for the Pacific and Indian ocean, *Pure Appl. Geophys.*, *166*, 301–324, doi:10.1007/s00024-008-0437-2.

A. Loevenbruck, CEA-DAM-DIF, Bruyères le Châtel, F-91297 Arpajon CEDEX, France. (anne.loevenbruck@cea.fr)

P. Lognonné, G. Occhipinti, and L. M. Rolland, Géophysique Spatiale et Planétaire, Institut de Physique du Globe de Paris, Université Paris Diderot, UMR CNRS 7154, 4 Ave. de Neptune, F-94100 Saint-Maur des Fossés CEDEX, France. (rolland@ipgp.fr)